

Nonclassical light from large ensembles of trapped ions

P. Obšil¹, L. Lachman¹, T. Pham², A. Lešundák², V. Hucl²,
M. Čížek², J. Hrabina², O. Číp², L. Slodička^{1*} and R. Filip¹

¹ *Department of Optics, Palacký University, 17. listopadu 12, 771 46 Olomouc, Czech Republic*

² *Institute of Scientific Instruments of the Czech Academy of Sciences,
Královopolská 147, 612 64 Brno, Czech Republic*

(Dated: February 5, 2022)

The vast majority of physical objects we are dealing with are almost exclusively made of atoms. Due to their discrete level structure, single atoms have proved to be emitters of light which is incompatible with the classical description of electromagnetic waves. We demonstrate this incompatibility for atomic fluorescence when scaling up the size of the source ensemble, which consists of trapped atomic ions, by several orders of magnitude. The presented measurements of nonclassical statistics on light unconditionally emitted from ensembles containing up to more than a thousand ions promise further scalability to much larger emitter numbers. The methodology can be applied to a broad range of experimental platforms focusing on the bare nonclassical character of single isolated emitters.

In 1905 Albert Einstein discovered that light can be understood as a stream of interfering photons [1]. At that time it was a contradiction to Maxwell's theory of light waves [2]. Quantum optics, however, merges our understanding of both wave and particle aspects together [3]. It seems to be commonly considered that light produced by large number of emitters is expected to be a mixture of classical waves [4]. This has been certified by a number of experiments analyzing various light sources from sun-light to laser radiation even with arbitrarily small intensity [5]. On the other hand, light from a single emitter with a transition between two discrete energy levels of atom or solid-state object is always nonclassical. Detection of an individual photon emitted from a single emitter cannot be described by a mixture of classical waves and therefore many results of single-photon experiments contradict classical coherence theory [6]. The most basic contradiction is observation of the indivisibility of a single photon at a beam splitter, which does not happen for classical light waves [7, 8]. However, the situation is already different for two photons as they can be split by linear optics. It is evident that ideal particle indivisibility typically manifested by measurement of perfect anti-bunching in the case of single-photon input is lost for a large number of photons even though some particle-like nonclassical features may remain. On the other hand, the state of a finite number of photons cannot be modelled as a mixture of classical waves, as those are always based on distributions of photons up to infinity. This particle-type of nonclassicality can remain hidden since the limitation in number of photons can be far away from what is detectable, as can be seen on classical sources consisting of enormous amounts of quantum emitters.

Observability of truly particle aspects of light therefore typically vanishes in everyday macroscopic reality and we frequently observe only mixtures of classical waves. This

is due to the inevitable enhancement of effects which deteriorate the macroscopic photon samples, but also affect their macroscopic sources and detectors. However, those effects are not fundamental and macroscopicity itself does not smudge the particle features. In order to succeed with the detection of particle-like nonclassical aspects of light for large number quantum emitters, the employed detection setup and evaluation procedure must provide unambiguous identification and sufficient information about nonclassical light without any prior assumptions. In addition, the measured light source needs to be stable in the number of photon emitters and the detection efficiency of unconditionally emitted light has to be sufficiently high to overcome the effects of background thermal noise. The detection apparatus and the employed criterion should be able to detect nonclassicality for a large number of photons in the presence of high loss, finite amplitude of added thermal noise and within feasible measurement times. These requirements have long forced the particle-like nonclassicality of radiation from large ensembles of emitters and its possible applications to remain in the domain of theoretical considerations. Apart from a few notable recent stimuli, which provide substantial evidence that nonclassicality is not necessarily bound to a few emitters [9, 10], experimental observations have been concerned by the analysis and control of nonclassical features on very small number of emitters. The ingenious fundamental questions considering the limits on the size of the particle samples and their number statistics, applicability of possible nonclassicality in large ensembles for detection of related fundamental effects like quantum phase transitions, particle entanglement, or its possible utilization for mesoscopic quantum computation still remain to be explored.

In this letter we present the experimental observation of nonclassical statistical properties of light emitted from large ensembles of single-photon emitters. We employ trapped ion crystals as a scalable source satisfying conditions for nonclassicality observability for large numbers of emitters. The recently proposed exactly measurable

*Electronic address: slodicka@optics.upol.cz

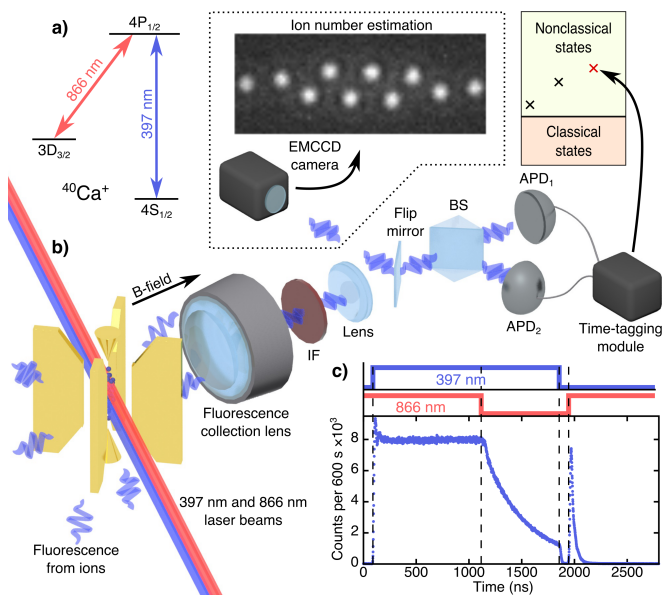


FIG. 1: The simplified scheme of experimental setup and laser pulse sequence for generation and detection of nonclassical light. a) The energy level scheme of the $^{40}\text{Ca}^+$ ion including employed transitions with their respective wavelengths. b) An ensemble of ions is trapped in the linear Paul trap and the 397 nm fluorescence emitted along the applied magnetic field direction (B-field) is collected by a lens objective and separated from the 866 nm light by an optical interference filter (IF). The fluorescence is then directed towards the nonclassicality analyzing setup comprising a single beam-splitter (BS), a pair of avalanche photodiodes (APDs) and the time-tagging module. The trapped ion crystals can be imaged on an EMCCD camera for the purposes of ion number estimation and optimization of trapping stability. c) The generation of analyzed light from the trapped ion ensemble in the pulsed regime begins by Doppler cooling period, in which both lasers are switched on. It is followed by the optical pumping stage, where the populations are shuffled to the metastable $3D_{3/2}$ state using only the 397 nm laser. The analyzed fluorescence at the $4P_{1/2} \leftrightarrow 4S_{1/2}$ transition is then generated by fast depopulation of the $3D_{3/2}$ state using the 866 nm laser pulse.

nonclassicality criterion, adjustable to the applied detection scheme [11], is used for witnessing the nonclassical character of emitted fluorescence. We measure the nonclassicality witness on emitted light for both pulsed and continuous laser excitation and verify the value of the nonclassicality threshold by conducting the same measurements with laser light.

Ensembles of large numbers of ions trapped in a Paul trap possess crucial advantages for initial proof-of-principle tests of nonclassicality [11, 12]. First, average trapping lifetimes of single ions in our setup exceed several days which allows for direct observation of emitted fluorescence even for very large ion numbers [13–16]. Second, laser cooled and trapped ion crystals can constitute isotopically pure samples of ions with lambda-type electronic level schemes. Due to their superb isolation

from environment and long trapping lifetimes, these systems have been employed for some of the pioneering tests of single-atom fluorescence nonclassicality [17, 18] and more recently, led to the demonstration of single-photon sources with record-breaking single-photon content [19–22]. Furthermore, the typical inter-atomic distance of ions in the traps is limited to be much larger than the wavelengths of the involved optical transitions due to the Coulomb repulsion, which suggests, that spontaneous build-up of collective effects can be neglected and ions can be treated as mutually independent emitters [23]. In addition, the ion trapping apparatus allows for near perfect control of the number of emitters in the crystal due to easily repeatable, albeit probabilistic ion-loading procedures.

In our measurements we focus on reaching the maximal number of participating ions while still unambiguously demonstrating the nonclassicality of the emitted light field allowed by practical limits related to the ion trapping and light collection apparatus. The simplified scheme of our experimental setup is shown in Fig. 1. The $^{40}\text{Ca}^+$ ion crystal is created by application of the trapping and Doppler-cooling forces in the potential minimum of a linear Paul trap. The light scattered from ions is collected using a lens covering $\approx 2\%$ of the full solid angle with the radial position and focal point carefully optimized for maximizing the fluorescence detection efficiency from a single ion trapped in the trap center. See Supplemental Material, Sec. A for more experimental details.

Nonclassical features of atomic fluorescence coming from trapped ion crystals are estimated by statistical analysis of the recorded time-tagged detection signal corresponding to exact times of photon arrival at the two avalanche photodiodes (APDs) using the criteria from Lachman et al. [11] based on the bare estimation of the true photon detection probabilities. These criteria fundamentally differ from the measures that incorporate moments of photon distribution including commonly employed nonclassicality estimation methods based on measurements of the intensity correlation function $g^2(\tau)$. The estimation of $g^2(\tau)$ corresponds to the measurement of the photon number variance, which cannot be safely realized when using binary single-photon detectors for observation of small nonclassicality from the large number of emitters. It generally requires the estimation of the whole photon number distribution. Although this is usually approximated by the probability of click and double click in the limit of small photon flux, such simplification is not safe in general and might become misleading especially when the number of emitters, and thus, number of emitted photons increases substantially [24, 25].

The employed criterion [11] includes the real response of single-photon detectors and takes into account possible unequal quantum detection efficiencies. It is operationally derived from first principles by construction of a linear functional depending on the probability of detecting no photon on both detectors, denoted P_{00} , and

no photon on one particular detector, denoted P_0 . The linear functional has the form

$$F_a(\rho) = P_0 + aP_{00}, \quad (1)$$

where a is a free parameter. If we consider a symmetrical detection scheme, optimizing $F_a(\rho)$ over all classical states $\rho = \int P(\alpha)|\alpha\rangle\langle\alpha|d^2\alpha$, where $P(\alpha)$ is a density probability function, leads to the threshold function $F(a) = -1/(4a)$ which covers all classical states. The nonclassicality condition requires a such that the detected probabilities satisfy $P_0 + aP_{00} > F(a)$. This a can be found if and only if $P_0 - \sqrt{P_{00}} > 0$. It thus allows for an unambiguous test of nonclassicality of light even with a high mean number of photons, where the approximation of moments by probabilities of clicks is not generally safe, because it can potentially imitate the nonclassical behaviour [26]. The nonclassicality is then witnessed by estimation of the probabilities within given time bin period and evaluation of the distance from the nonclassicality threshold

$$d = P_0 - \sqrt{P_{00}} > 0. \quad (2)$$

We note, that the parameter d by no means gives a quantitative measure of nonclassicality, it is solely a suitable witness for nonclassical states from the large ensembles of emitters. The parameter d can be equivalently defined also in terms of the probability of a click P_s and a double click P_c , see Supplementary Information D for more details. However, the parameter d is better for understanding the experiments with many emitters. The value of d increases with the number of contributing single-photon emitters while it is non-increasing if noise, Poissonian or thermal, is added instead [11]. The $g^2(0)$ does not provide such information directly, as it converges to unity for addition of both single-photon emitters and noise sources.

We measure the statistics of emitted fluorescence in both pulsed and continuous excitation regimes, which effectively represent different sources of radiation. In the continuous case, ions in the crystal emit fluorescence at random and mutually uncorrelated times and, in principle, finite linewidth of the employed transition and laser light leakage can result in multiple emissions from a single ion within the same time bin. This is well illustrated by the decreased purity of the single photons emitted from single atoms estimated from measurements of intensity correlation functions $g^2(0)$ in continuous schemes compared to pulsed sources, in which the multiphoton emission is typically prohibited by the optical pumping mechanism [19–22]. The pulsed driving is thus much more convenient for demonstration of the nonclassical emission from large atomic ensembles, provided that the rate of the photon emission given by pulse sequence length can be kept comparably high. As can be seen in Fig. 1-a) and 1-c), we employ an effectively three-level energy structure of the $^{40}\text{Ca}^+$ to minimize the multiphoton content in the given measurement time-bin by optically pumping the atomic population to the metastable

$3D_{3/2}$ level from where the photon emission is initiated by the 866 nm laser pulse. The optical pumping characteristic time is relatively long for our excitation parameters and crystal spatial extensions, and depending on the laser settings, about one fifth of emitters remain in the $4S_{1/2}$ level. The efficiency of the optical pumping to the $3D_{3/2}$ manifold is estimated from the observed fluorescence rates in the pulsed photon generation sequence, see the example in the Fig. 1-c). The residual average detected photon rate at the end of the 397 nm pulse is compared with the value of the photon rate during the Doppler cooling period, which gives a lower bound on the $3D_{3/2}$ population. The exact value can be then estimated by evaluating the steady state populations of the $3D_{3/2}$ state for given Doppler cooling laser excitation parameters. The single-photon detectors are gated with the gating time optimized to comprise most of the generated 397 nm light. The detailed description of measured data processing can be found in Supplemental Material, Sec. B.

The evaluated value of witness d defined in Eq. (2) for trapped ion crystals containing from one to up to several hundreds of ions is plotted in Fig. 2-a). A clear violation of the nonclassicality condition by several error bars marking single standard deviation is observed for all ion numbers up to 275 in both continuous and pulsed regimes. The corresponding theoretical prediction of the parameter d in the pulsed regime has been evaluated and plotted by taking into account the measured distribution of detection efficiencies for ions in the given crystal. The theoretical prediction agrees well with the measured data, even without any free fitting parameter and without taking into account experimental imperfections like the optical pumping spatial distribution, or intensity fluctuations of the exciting lasers. In the presented simulation, we have considered the ion crystals with concentric shell structure supported by our observations. Details of the simulation can be found in Supplemental Material, Sec. C. The ion storage lifetime and crystal stability can play a crucial role for the statistical properties of the emitted light. We have analyzed the rate of loss of ions in our setup in the regime where the cooling lasers frequencies are locked and the trap input radio-frequency power remains stable. The number of trapped ions was precisely counted before and after each photon-counting measurements and there has been no observable loss of ions in the presented measurements. We note, that only 2 out of 14 measurement runs were discarded due to loss of ions caused by cooling laser frequency instability. For comparison, the quality of our single-photon emitter-single ion has also been evaluated using the conventional measure based on the estimation of the intensity correlation function $g^2(0)$, which gives $g^2(0) = 0.081$ in the continuous case for a 1 ns time bin and $g^2(0) = 0.032$ in the pulsed excitation regime, comparable to other realizations of single-photon sources with single trapped ions [19–22].

The internal atomic dynamics and multi-photon con-

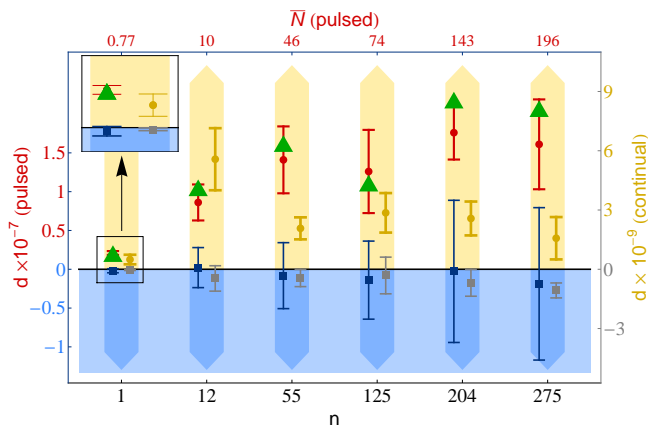


FIG. 2: The measured violation of nonclassicality as a function of the number of trapped single-photon emitters and the same measurements realized just with the laser light. All measured values of the witness d for trapped ion ensembles in pulsed (red circles) and continuous (yellow circles) regimes are provably in the nonclassical region given by $d > 0$. The green triangles correspond to the numerical simulation of the witness value in the pulsed regime, details of the simulation can be found in Supplemental Material, Sec. C. Estimated mean photon numbers per single emission pulse \bar{N} in the pulsed regime are shown on the top axis. d for the 397 nm laser light scattered from the trap electrodes has been measured using the same detection scheme in both excitation regimes. The laser intensity has been set to reach the detection count-rates corresponding to measurement on light from a given trapped ion ensemble. The dark blue and grey squares are measurements on the laser light in the pulsed and continuous regimes, respectively. All measurements corresponding to a given ion number are grouped in arrow-like shaded regions. Error bars correspond to one standard deviation.

tributions make it difficult to theoretically predict the measured parameter d in continuous regime. The actual uncertainty in the emission time and possibility of multiphoton contributions from single atoms within finite time bins make this regime closer to a large class of optical sources with uncontrolled internal dynamics or partial coupling to environment [27] and the presented measurements will likely stimulate investigations of their statistical properties.

The technical limit on further increasing the number of emitters in our experiment is given by the effective detection volume of the employed optical detection setup. The photon detection efficiency falls rapidly for ions positioned in the radial direction from the collection lens focal point and less rapidly, but still considerably, along the lens symmetry axis. See Supplemental Material, Sec. A for more details. The limiting radial size of the detection volume for our detection arrangement is $4.6 \mu\text{m}$ (FWHM). The detection efficiency variation at various distances from the lens focal point suggests that increasing the measured crystal size beyond hundreds of ions in our setup inevitably places some of them into re-

gions with extremely small relative collection efficiency. The transition to small relative detection efficiencies is smooth in all three spatial directions, which brings in a technical question of how many emitters actually substantially contribute to the detected photon flux. This fuzziness in the number of contributing emitters is seen as a sign of dealing with a system which approaches the fragile borderline between the applicability of quantum and classical descriptions, at which the suitability of the discrete quantum description of some important physical variables, like number of emitters or total energy, naturally deteriorates. The mere technical limit of the employed optical detection setup can be eliminated by the use of optimized imaging configurations. We demonstrate further scalability of the nonclassicality measurements in similar setups by changing the lens configuration so that we decrease its overall magnification factor, which corresponds to an increase of the radial detection volume. We reach a radial field of view of approximately $20 \mu\text{m}$ without observing any substantial change of the absolute detection efficiency of an ion positioned on the optical axis. With this configuration, we have measured the positive distance $d = (9.48 \pm 3.93) \times 10^{-7}$ for 1500 ± 200 ions in an equal 5 hour long experimental run. We note, that this would correspond to 391 ions when considering only emitters contributing to the detected optical signal with relative efficiency higher than η_{max}/e , where η_{max} is the overall detection efficiency for an ion positioned at the optical axis of the employed detection system and e is Euler's number.

The photon flux per single emission pulse at the input of the detection apparatus has been estimated for each measurement in the pulsed regime from the number of trapped ions n and measured finite efficiency of the optical pumping η_p as $\bar{N} = n \times \eta_p$. The highest mean photon number at the input of our detection apparatus is $\bar{N} = 196$ photons, which correspond to $n = 275$ ions and $\eta_p = 71\%$ optical pumping efficiency. To the best of our knowledge, this corresponds both to the largest ensemble of single-photon emitters and the largest photonic field for which nonclassical statistical properties have been demonstrated. Furthermore, as can be seen in Fig. 2-a), the relative uncertainty of the measurements of the distance d scales very favorably with number of ions, which promises scalability of our measurements to much higher ion numbers, provided that the emitted light is collected efficiently.

Furthermore, there seems to be no fundamental limit on further substantial increase of any of these quantities in a similar experimental apparatus. We have simulated the emission of light from a crystal containing up to 10^5 ions. The simulation predicts scaling of the parameter d and uncertainty caused by finite measurement with size of the crystal. As already predicted in Ref. [11], the main limiting parameter for unambiguous detection of nonclassicality for stable ensembles of single-photon emitters is the measurement time. The detailed analysis presented in Supplemental Material, Sec. C shows,

that the required experimental time does not grow substantially until the mean photon flux at photo-detectors reaches several photons. The nonclassicality of stronger light would be also observable, however it would require additional attenuation to reach the optimal photon flux for measuring nonclassical properties.

The presented measurements demonstrate the first unambiguous proof of the nonclassical character of light fields emitted from a large ensemble of single-photon emitters. We have shown that ensembles consisting of emitters which individually produce nonclassical light, keep this statistical property when scaling up their size by at least two orders of magnitude by trapping and measuring for a range of ion numbers, from a single ion up to 275 ions. Moreover, the demonstrated nonclassicality measurements present robustness against many imperfections of individual sources. We have also verified several aspects of emission from ensemble of single-photon sources compared to emission from a single one. Most notably the measured nonclassicality witness value in the pulsed regime grows or stays approximately constant with increasing emitter number.

Our experimental test opens the possibility of searching for nonclassical light emission from recently developed ensembles of atomic [28, 29] and solid-state emitters [9, 10] and studying their internal dynamics from a new perspective [30–32]. It will allow their exploration before single emitters are isolated and further direct exploitation in quantum technology [33]. Furthermore, due to the large dependence of the ability to detect nonclas-

sicality on the statistics of emitters and emitted light mode-structure stability, the presented scheme can be easily applied for detection of phase transitions from solid to gas or plasma phase [32]. The presented demonstration can be directly extended in the future to ion numbers beyond thousands by employing optimized optical fluorescence collection schemes, and later, to observations of emissions going toward the Fock states of indistinguishable photons from atoms inside a cavity [34, 35]. It substantially shifts the range of energies in which observable manifestations of discrete quantum features of light and matter should be anticipated and thus will likely trigger the construction of truly macroscopic and intense sources of quantum light.

In the course of preparing our manuscript we became aware of another experiment studying nonclassicality from ensembles of single-photon emitters [36]. It demonstrates the applicability of the presented proof-of-principle methodology for studies of emission from clusters of NV centers in diamond and its robustness against realistic sources of noise.

Acknowledgments

The work reported here has been supported by the grant No. GB14-36681G of the Czech Science Foundation. We acknowledge the kind technological support from the group of Rainer Blatt.

-
- [1] A. Einstein, *Annalen der Physik* **322**, 132 (1905).
 - [2] J. C. Maxwell, *Philosophical Transactions of the Royal Society of London* **155**, 459 (1865).
 - [3] L. Mandel and E. Wolf, *Optical Coherence and Quantum Optics* (Cambridge University Press, 1995).
 - [4] R. J. Glauber, *Quantum Theory of Optical Coherence: Selected Papers and Lectures* (Wiley-VCH, 2007).
 - [5] P. K. Tan, G. H. Yeo, H. S. Poh, A. H. Chan, and C. Kurtzinger, *The Astrophysical Journal Letters* **789**, L10 (2014).
 - [6] M. Born and E. Wolf, *Principles of Optics: Electromagnetic Theory of Propagation, Interference and Diffraction of Light* (Cambridge University Press, 2002).
 - [7] H. J. Kimble, M. Dagenais, and L. Mandel, *Physical Review Letters* **39**, 691 (1977).
 - [8] P. Grangier, G. Roger, and A. Aspect, *Europhysics Letters* **1**, 173 (1986).
 - [9] O. A. Shcherbina, G. A. Shcherbina, M. Manceau, S. Vezoli, L. Carbone, M. De Vittorio, A. Bramati, E. Giacobino, M. V. Chekhova, and G. Leuchs, *Optics Letters* **39**, 1791 (2014).
 - [10] L. J. Rogers, K. D. Jahnke, T. Teraji, L. Marseglia, C. Müller, B. Naydenov, H. Schauffert, C. Kranz, J. Isoya, L. P. McGuinness, and F. Jelezko, *Nature Communications* **5**, 4739 (2014).
 - [11] L. Lachman, L. Slodička, and R. Filip, *Scientific Reports* **6**, 19760 (2016).
 - [12] R. Filip and L. Lachman, *Physical Review A* **88**, 043827 (2013).
 - [13] R. W. Hasse and V. V. Avilov, *Physical Review A* **44**, 4506 (1991).
 - [14] M. Drewsen, C. Brodersen, L. Hornekær, J. S. Hangst, and J. P. Schiffer, *Physical Review Letters* **81**, 2878 (1998).
 - [15] H. Totsuji, T. Kishimoto, C. Totsuji, and K. Tsuruta, *Physical Review Letters* **88**, 125002 (2002).
 - [16] K. Okada, M. Wada, T. Takayanagi, S. Ohtani, and H. A. Schuessler, *Physical Review A* **81**, 013420 (2010).
 - [17] F. Diedrich and H. Walther, *Physical review letters* **58**, 203 (1987).
 - [18] M. Schubert, I. Siemers, R. Blatt, W. Neuhauser, and P. E. Toschek, *Physical review letters* **68**, 3016 (1992).
 - [19] D. B. Higginbottom, L. Slodička, G. Araneda, L. Lachman, R. Filip, M. Hennrich, and R. Blatt, *New Journal of Physics* **18**, 093038 (2016).
 - [20] P. Maunz, D. Moehring, S. Olmschenk, K. C. Younge, D. N. Matsukevich, and C. Monroe, *Nature Physics* **3**, 538 (2007).
 - [21] C. Kurz, J. Huwer, M. Schug, P. Müller, and J. Eschner, *New Journal of Physics* **15**, 055005 (2013).
 - [22] H. G. Barros, A. Stute, T. E. Northup, C. Russo, P. O. Schmidt, and R. Blatt, *New Journal of Physics* **11**, 103004 (2009).
 - [23] R. G. Brewer, *Physical Review A* **53**, 2903 (1996).
 - [24] R. Short and L. Mandel, *Physical Review Letters* **51**, 384

- (1983).
- [25] M. Avenhaus, K. Laiho, M. V. Chekhova, and C. Silberhorn, *Physical Review Letters* **104**, 063602 (2010).
 - [26] J. Sperling, W. Vogel, and G. S. Agarwal, *Physical Review A* **85**, 023820 (2012).
 - [27] A. Predojević, M. Ježek, T. Huber, H. Jayakumar, T. Kauten, G. S. Solomon, R. Filip, and G. Weihs, *Optics Express* **22**, 4789 (2014).
 - [28] T. E. Northup and R. Blatt, *Nature Photonics* **8**, 356 (2014).
 - [29] A. Neuzner, M. Körber, O. Morin, S. Ritter, and G. Rempe, *Nature Photonics* **10**, 303 (2016).
 - [30] D. Bhatti, J. Von Zanthier, and G. S. Agarwal, *Scientific Reports* **5**, 17335 (2015).
 - [31] F. Jahnke, C. Gies, M. Aßmann, M. Bayer, H. Leymann, A. Foerster, J. Wiersig, C. Schneider, M. Kamp, and S. Höfling, *Nature Communications* **7**, 11540 (2016).
 - [32] L. Hornekær and M. Drewsen, *Physical Review A* **66**, 013412 (2002).
 - [33] C. Palacios-Berraquero, D. M. Kara, A. R.-P. Montblanch, M. Barbone, P. Latawiec, D. Yoon, A. K. Ott, M. Loncar, A. C. Ferrari, and M. Atatüre, *Nature Communications* **8**, 15093 (2017).
 - [34] B. Casabone, K. Friebe, B. Brandstätter, K. Schüppert, R. Blatt, and T. E. Northup, *Physical Review Letters* **114**, 023602 (2015).
 - [35] C. Sayrin, I. Dotsenko, X. Zhou, B. Peaudecerf, T. Rybarczyk, S. Gleyzes, P. Rouchon, M. Mirrahimi, H. Amini, M. Brune, J.-M. Raimond, and S. Haroche, *Nature* **477**, 73 (2011).
 - [36] E. Moreva, P. Traina, J. Forneris, I. P. Degiovanni, S. D. Tchernij, F. Picollo, G. Brida, P. Olivero, and M. Genovese, *Physical Review B* **96**, 195209 (2017).

Supplementary information: Nonclassical light from large ensembles of trapped ions

A. Experimental setup

Ion trapping

The trap parameters are set with respect to maximizing the stability of a particular ion crystal and the number of detected photon counts. This corresponds to close to symmetrical configuration of oscillation frequencies of the trapping potential $\omega_x \approx \omega_y \approx \omega_z \approx 778$ kHz for measured ion crystals containing more than 12 ions, and configuration with $\omega_x \approx \omega_y \approx 1341$ kHz and $\omega_z \approx 778$ kHz for measurements with 1 and 12 ions. Here, ω_z is the frequency of the trapping potential in the axial direction of the trap, that is, along the axis connecting the two tip electrodes, and the ω_x, ω_y are the frequencies of the potential in the radial directions which lie in the plane perpendicular to the axial direction. The measured ion ensembles with more than 12 ions correspond to near spherical crystals with concentric shell structure [S1–S3], which have been chosen to optimize the overall scattered light collection efficiency in the direction perpendicular to the trap axis. The ions are Doppler cooled by a red detuned 397 nm laser exciting the $4S_{1/2} \leftrightarrow 4P_{1/2}$ transition and a 866 nm laser beam is simultaneously used for repumping the population from the metastable $3D_{3/2}$ state to the cooling transition. A magnetic field of 12 Gauss is applied along the observation direction to lift the degeneracy of the $3D_{3/2}$ state manifold and thus enable its effective depopulation. The excitation beams are co-propagating in the direction perpendicular to the magnetic field direction with linear polarization parallel to it.

Light detection

The light scattered from an ensemble of ions is collected by an objective covering $\sim 2\%$ of the full solid angle and frequency filtered (IF) to isolate the 397 nm fluorescence. The photons are then directed towards one of two possible detection arrangements. The EMCCD camera (Luca-S, Andor) is used for spatial analysis of the trapped ion crystal, estimation of the number of emitters before and after each experimental run, and further calibration measurements, including estimation of the excess micromotion of off-axis positioned ions and photon emission probability homogeneity across the crystal. The light is further split by a beamsplitter (BS) and directed towards a pair of free-space-coupled avalanche photodiodes (APDs, Count-series, Laser Components). The overall detection efficiencies of fluorescence emitted by the ion positioned in the focus of the collection lens have been estimated to be 0.033% and 0.028%, for the APD₁ and APD₂, respectively. Precise arrival times of incoming photons are recorded (PicoHarp300, PicoQuant) with time resolution of 4 ps

and further processed to obtain the individual photon detection probabilities. The measured detection efficiencies fall down rapidly for ions displaced radially from the collection objective focal point due to the limited field of view of the whole detection setup, which gives the limit on the number of effectively coupled ions. We have separately estimated detection efficiencies for ions displaced in radial and axial directions. In the radial direction of the lens object plane, which corresponds to ion displacement along the trap axis, the measured detection efficiencies of single photons scattered from a single ion normalized to the efficiency in the center yield an approximately Gaussian efficiency profile with a full width at half maximum (FWHM) of $4.6 \mu\text{m}$, see Fig. S1-a). This relatively narrow radial field of view of the employed detection setup is given by the magnification of our detection optics and size of the active detector area. The effective image area is given by the magnification and optical aberrations of the employed optical detection setup consisting of the high-NA objective with object focal distance of approximately 66 mm and an additional 400 mm plano-convex lens together with the finite active detection area of the APD of about 100 microns. In the axial direction, the effective ion displacement has been emulated by the collection objective axial displacement using precise translation stage. The measured decrease of the relative detection efficiency is plotted in Fig. S1-b). The FWHM of the fitted Gaussian function is 238 microns. As can be seen in Fig. S1-c), this detection limitation manifests as small relative contributions of ions positioned far from the detection optical axis.

Pulsed and continuous modes of excitation

Measurements of nonclassicality of light emitted from ion crystals are realized in both continuous and pulsed regimes, which substantially differ in properties of emitted light and in the technical feasibility of its detection with single photon detectors with finite detection bandwidth. We have evaluated this difference by comparison of the $g^2(0) = 0.081$ in the continuous case for a 1 ns time bin with $g^2(0) = 0.032$ in pulsed excitation.

General remarks

The particular excitation parameters in the continuous regime give us at maximum up to 36900 counts/s and 31500 counts/s on APD₁ and APD₂ detectors, respectively, far from the detector saturation rates, which are specified to be approximately in the 10^6 counts/s regime.

B. Data processing

Measurement and evaluation of the d parameter

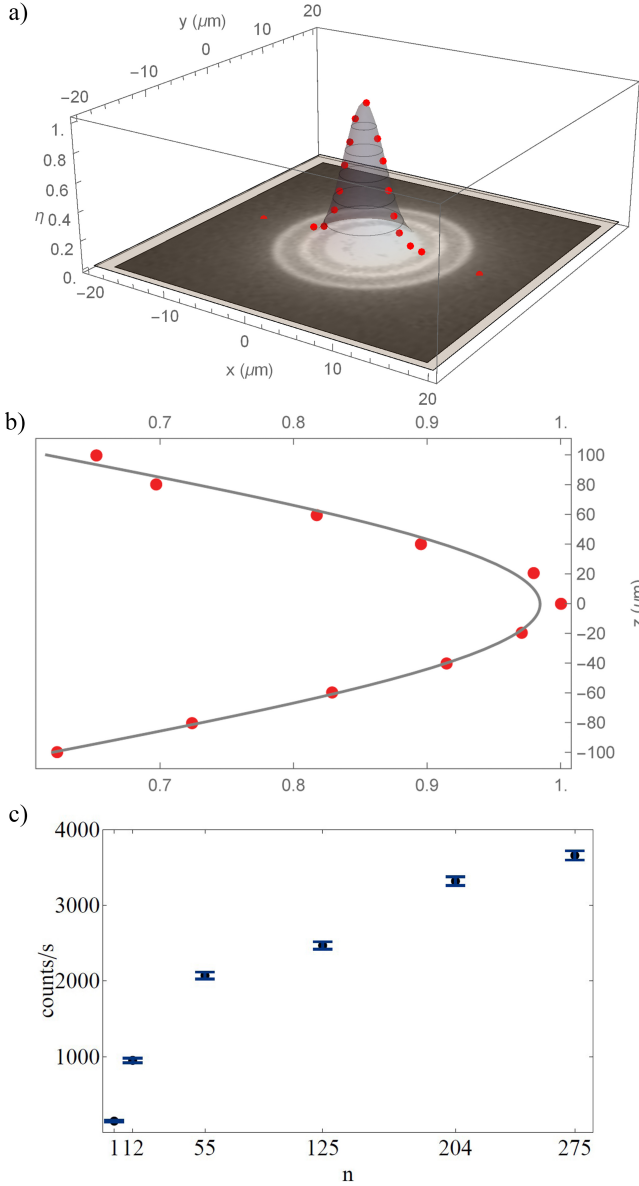


FIG. S1: The estimation of the effect of finite detection volume by the measurement of detection efficiencies in the radial and axial object planes and evaluation of the overall detected count rate for trapped ion ensembles. In a) we show relative detection efficiencies normalized to the maximal efficiency corresponding to the lens on-axis position. The bottom plane of the 3D figure is filled with the picture of the ion crystal consisting of $n = 275$ ions scaled to correct units. The graph in b) shows measured efficiencies for the ions effectively displaced along the lens axis for the displacements relevant for the spatial sizes of the measured ion crystals. The fitted Gaussian function has FWHM of 238 microns. The dependence of the detected count rate on the number of ions n shown in part c) in the pulsed regime demonstrates the effect of decreased overall detection efficiency of light emitted far from the collection objective optical axis.

The fluorescence from the ion ensemble is detected using two APDs and the arrival times of scattered photons are recorded using time-tagged device with 4 ps resolution. Further processing has two parts, manipulation with raw time-tagged data for estimation of probabilities P_{00} and P_0 , and estimation of nonclassicality with corresponding uncertainties. In the first step, we start by evaluation of the total number N_{TB} of all time-bins of size τ in a given measurement, N_C number of events where both APDs register a photon in the same time-bin and N_{S1} and N_{S2} , which correspond to events where APD₁ and APD₂ register a photon, respectively. While in the continuous regime we need to cut the time arrival data to time-bins, in the pulsed measurements processing is one step easier, because each sequence includes the APD gating pulse which corresponds to a single time-bin. We further shorten this time-bin in the data processing step in order to remove the false clicks due to the APD gating pulses, which otherwise correspond to about 10% of real photon detection events depending on the mean input photon flux. According to the employed criterion of nonclassicality, we need to estimate the probabilities P_{00} and P_0 . The measured photon detection numbers are related to these probabilities through the following relationships:

$$P_{00} = \frac{N_{\text{TB}} - N_{S1} - N_{S2} - N_C}{N_{\text{TB}}}, \quad (\text{S1})$$

$$P_{0k} = \frac{N_{\text{TB}} - N_{S_k} - N_C}{N_{\text{TB}}} \quad (\text{S2})$$

and

$$P_0 = \sqrt{P_{01} \cdot P_{02}}, \quad (\text{S3})$$

where the use of the geometrical mean is due to a slight imbalance between the absolute detection efficiencies in our detection apparatus. The use of the geometrical mean here is justified by the following consideration. For a known imbalance T of the detection efficiencies, nonclassicality is witnessed if at least one of the following conditions is satisfied [S4]

$$P_{01} > P_{00}^T \quad (\text{S4})$$

$$P_{02} > P_{00}^{1-T}. \quad (\text{S5})$$

Multiplying left and right sides of those inequalities excludes T and leads directly to

$$P_{01} \cdot P_{02} > P_{00}. \quad (\text{S6})$$

It is obvious, that if this relation holds, at least one of these inequalities has to be satisfied, which guarantees the nonclassicality.

From P_0 and P_{00} we estimate nonclassicality of the measured light field using the equation (2) from the main

part of the manuscript. The error bars are estimated statistically by dividing our 5 hour long measurement into 5 parts of equal length for which the nonclassicality has been estimated independently.

Statistical evaluation of the measured results

We have statistically evaluated the behaviour of the d parameter as a function of the number of emitters in our experiment measured in the pulsed excitation regime. We have performed comparisons of individual d values together with the measured error propagation with the following results. $d(1) < d(12)$ with the confidence level of 99.9% and $d(12) < d(55)$ with the confidence level of 99% which means that the value of d clearly grows up to 55 ions. The comparisons between measurements of d for number of ions $n \geq 55$ are, from point to point, not conclusive with similarly high confidence levels mainly due to relatively large error bars compared to the difference in their mean values. However, one can still give a statistical estimate on the validity of the overall rising trend by estimation of the mean gradient of the weighted linear fit and its error. This analysis confirms the observation of further increase of d in the presented measurements for number of ions $n \geq 55$. The value of d increases with the number of ions in the range $n \geq 55$ with a confidence level of 87%.

C. Simulations

Estimation of the theoretical distance for our experimental setup

Although the source of light consisting of trapped ions is a very complex system with a large number of inner parameters, one can capture the properties of the emerging light using several simplifying assumptions about the physics behind. First, each ion is treated as an ideal single photon emitter whose emission is independent of the presence or state of other ions. This means that the light is radiated independently. The cooling of the ions causes formation of the ion crystal. The crystal in our measurement has spherical symmetry (except the crystal with 12 ions) and a shell structure. The numbers of ions in different shells are obtainable by simulation of molecular dynamics [S5]. The occupation of shells in our crystals is following: a crystal with 12 ions is formed only in one shell, a crystal with 55 ions has two shells (12+43 ions), a crystal with 125 ions has three shells (82+35+8 ions), a crystal having 204 ions consists of four shells (115+60+25+4 ions), and a crystal with 275 also has four shells (150+80+36+9 ions). According to the numerical model from [S5], the spacing among particular shells is almost constant. Additionally, we suppose that ions within shells have no crystal structure but rather correspond to a gaseous or plasma state with homogeneous but random distribution in each shell [S1, S3, S5]. This assump-

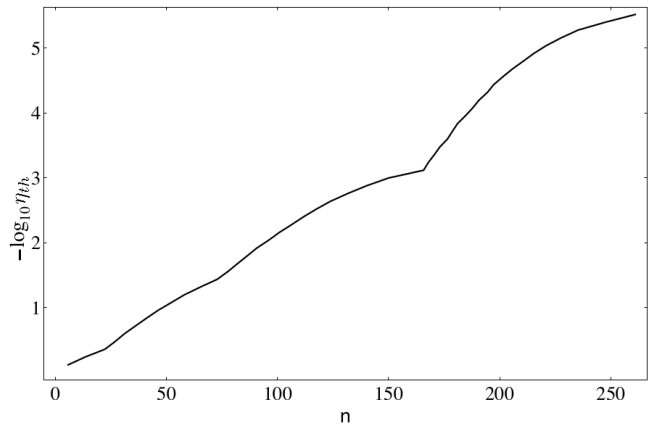


FIG. S2: Simulation of number of contributing emitters n with the efficiency higher than relative threshold efficiency $\eta_{th} = \eta/\eta_0$ and for the crystal containing 275 ions.

tion is supported by our measurements of ion ensemble images on EMCCD camera. To simulate this random distribution, we choose several polyhedra carrying some symmetry whose vertices, after random rotation, determine the position of ions on a shell. Therefore the simulation requires a sufficient number of random rotations of each polyhedron to obtain a homogenous distribution of vertices. The employed polyhedra are a tetrahedron (four vertices), a cube (8 vertices), a regular icosahedron (12 vertices), a regular dodecahedron (20 vertices) and a truncated icosahedron (60 vertices). To simulate a shell with an arbitrary number of ions, we can combine these polyhedra and randomly delete a few vertices to adjust the total vertices to the desired number.

If the ions are excited, they act as single photon emitters radiating photons by spontaneous emission in directions defined by a given dipole radiation pattern. However, the lens is able to collect and focus on detectors only a small part of this emission. This, together with quantum efficiency of the detectors, yields an overall detection efficiency $\eta_0 = 6.1 \cdot 10^{-4}$ for the emitters situated in the object focal point of the whole detection optical setup. As demonstrated in measurements presented in Supplementary information A, emitters positioned out of the focus are less likely to be observed due to decreased detection efficiency. We assume that the detection efficiency depends on position as

$$\eta = \eta_0 \cdot e^{-\frac{r^2}{2\sigma_r^2} - \frac{a^2}{2\sigma_a^2}} \quad (S7)$$

where r is the distance from the optical axis of the lens and a is the distance from the focal plane. σ_r and σ_a correspond to variances of this Gaussian distribution. We have experimentally estimated their values $\sigma_r = 2.3 \mu\text{m}$ and $\sigma_a = 98 \mu\text{m}$. It suffices to use only one crystal for the calibration of the spatial size in the simulation, because the ratio of the number of ions in a crystal to its volume is approximately constant [S5]. Significantly, this

approach assigns statistics of detector clicks to a crystal having n ions. The probabilities P_{00} and P_0 employed in our criterion of nonclassicality are obtained by $P_{00} = \prod_{i=1}^n (1 - \eta_i)$ and $P_0 = \prod_{i=1}^n (1 - \eta_i/2)$. This enables us to plot the estimate of parameter d for crystals in our measurement as depicted in Fig. 2 in the main part of the manuscript. The largest crystal in these measurements contained $n = 275$ ions. However, as described in Supplementary information A, not all emitters contributed equally to the detected light. The measured detection efficiencies as a function of radial ion displacement show that increase of the measured crystal size beyond approximately one hundred ions inevitably places some of them into the regions with very small relative detection efficiency. This gives rise to questions about the lowest detection efficiency of an ion, which is still relevant for the observed light statistics, relative to the ion with maximal detection efficiency. Because it cannot be answered generally, we estimate the number of ions from which photons are detected with probability above some value, see Fig. S2. Apparently, the narrow volume of the lens significantly suppresses detection of photons emitted from outer shelves of the crystal.

Prospect of measurements on higher number of trapped ions

The theoretical prediction of visibility of nonclassicality for higher photon flux requires both the estimation of the parameter d and a corresponding uncertainty that stems from the fluctuation of experimental outputs (S1) and (S2). Let us introduce a linear combination of the measured quantities and their mean values

$$\begin{aligned} X &= 2P_0 - P_{00} \\ Y &= P_0 + 2P_{00} \\ x &= \langle X \rangle \\ y &= \langle Y \rangle. \end{aligned} \quad (\text{S8})$$

The probability density function of random quantities X and Y is approximated in the limit of a high number of experimental runs by Gaussian distribution

$$P(X, Y) = \frac{1}{2\pi\sqrt{V_x V_y}} \exp \left[-\frac{(X - x)^2}{2V_x} - \frac{(Y - y)^2}{2V_y} \right], \quad (\text{S9})$$

where $V_{x,y}$ is the variance of the variable X, Y . These quantities are related to detection events such that

$$\begin{aligned} \langle X \rangle &= 1 - P_c \\ \langle Y \rangle &= \frac{1}{2}P_s + \frac{3}{2}P_{00}, \end{aligned} \quad (\text{S10})$$

where P_c is a probability of a coincidence click and P_s means probability of just a single click. Thus, the variances obey

$$\begin{aligned} V_x &= \frac{P_c(1 - P_c)}{N} \\ V_y &= \frac{P_s(1 - P_s)}{4N} + \frac{9P_{00}(1 - P_{00})}{4N}. \end{aligned} \quad (\text{S11})$$

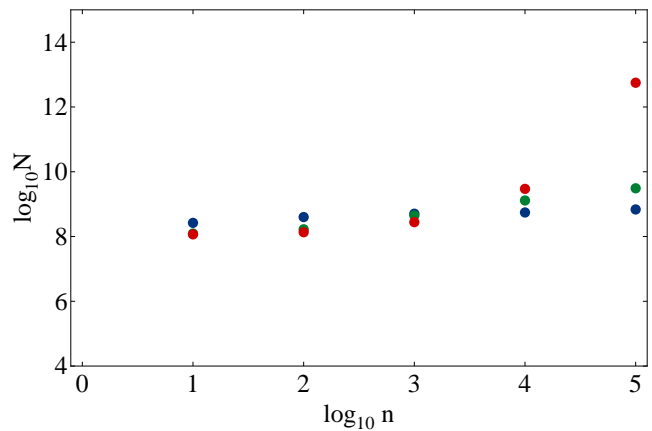


FIG. S3: The number N of experimental runs necessary to violate the nonclassicality by two errorbars is depicted for crystals counting n ions. The parameters of the detection are $\eta = 4 \times 10^{-4}$ and $\sigma_a = 98 \mu\text{m}$. Different colors correspond to $\sigma_r = 2 \mu\text{m}$ (blue), $\sigma_r = 8 \mu\text{m}$ (green) and $\sigma_r = 20 \mu\text{m}$ (red).

The parameter d is given by

$$d = \frac{2X + Y}{5} - \sqrt{\frac{-X + 2Y}{5}}. \quad (\text{S12})$$

The probability density function (S9) enables us to obtain

$$\text{var}(d) = V_x \left(\frac{\sin \phi}{2\sqrt{p_{00}}} + \cos \phi \right)^2 + V_y \left(\frac{\cos \phi}{2\sqrt{p_{00}}} - \sin \phi \right)^2, \quad (\text{S13})$$

where $\phi = \arctan 1/2$. For very weak light sources, one gets $\text{var}(d) \approx 0.315P_c/N \ll \text{var}(P_0)$, which indicates that the measured point fluctuates mainly in the direction parallel with the curve corresponding to the nonclassicality threshold.

The shell structure of a crystal simulated in [S5] is presented completely for crystals containing up to 2000 ions. Crystals with a higher number of ions tend to change the arrangement of ions to a bcc grid [S6]. The Cartesian coordinates of emitters in the bcc grid are given by the formulas

$$\begin{aligned} x_i &= iu + \frac{1}{4} [-(-1)^j + 1] u \\ y_j &= j \frac{\sqrt{3}}{2} u + \frac{1}{2\sqrt{3}} u [-(-1)^k + 1] \\ z_k &= k \sqrt{\frac{2}{3}} u, \end{aligned} \quad (\text{S14})$$

where u is the distance between two ions and i, j and k are integers. To emphasize further scalability of our measurements, we analyze the number of experimental runs necessary for violation of nonclassicality by two standard deviations, see Fig. S3.

D. Nonclassicality criterion

The employed condition on nonclassicality [S7] has been derived ab initio without any assumptions about the state of the detected light and can be equivalently defined in terms of the probability of a click P_s and a double click P_c . The condition for the symmetric detection technique then says $P_c/P_s^2 < 1$. In this symmetric case, the ratio on the left side of the inequality converges to $g^{(2)}$ but it is never the same. In addition, the criterion

can be advantageously formulated for any asymmetry of the detectors and can fully incorporate known structure or properties of the employed realistic detector. Importantly, it also allows a choice of the suitable parametrization for the analysis. The advantage of the particular selected parametrization by probabilities P_0 and P_{00} is a very simple theoretical proof that an arbitrarily large ensemble of single photon emitters generates nonclassical light [S7].

-
- [S1] M. Drewsen, C. Brodersen, L. Hornekær, J. S. Hangst, and J. P. Schiffer, *Physical Review Letters* **81**, 2878 (1998).
- [S2] L. Hornekær and M. Drewsen, *Physical Review A* **66**, 013412 (2002).
- [S3] K. Okada, M. Wada, T. Takayanagi, S. Ohtani, and H. A. Schuessler, *Physical Review A* **81**, 013420 (2010).
- [S4] R. Filip and L. Lachman, *Physical Review A* **88**, 043827 (2013).
- [S5] R. W. Hasse and V. V. Avilov, *Physical Review A* **44**, 4506 (1991).
- [S6] H. Totsuji, T. Kishimoto, C. Totsuji, and K. Tsuruta, *Physical Review Letters* **88**, 125002 (2002).
- [S7] L. Lachman, L. Slodička, and R. Filip, *Scientific Reports* **6**, 19760 (2016).